

# Microstructure and Mechanical Properties of Ceramic/Self-Assembled Monolayer Bilayer Coatings

K. CHITRE,<sup>1</sup> Q. YANG,<sup>1</sup> T.O. SALAMI,<sup>2</sup> S. R. OLIVER,<sup>2</sup> and J. CHO<sup>1,3</sup>

1.—Department of Mechanical Engineering, State University of New York at Binghamton, Binghamton, NY 13902-6000. 2.—Department of Chemistry, State University of New York at Binghamton. 3.—jcho@binghamton.edu

Thin ceramic coatings/films find their applications in various electronic devices, sensors, and microelectromechanical systems (MEMS) as a protection/barrier layer as well as functional films. Ceramics are, however, susceptible to catastrophic failure due to their inherent brittleness. We have developed a strain-tolerant, bilayer coating consisting of a ceramic layer and a self-assembled monolayer (SAM). The top ceramic coating offers an inert, protective layer, while the underlying SAM acts as a “template” for the subsequent growth of a hard ceramic coating. In this study, we explore the ZrO<sub>2</sub>/SAM coatings on Si substrates prepared *in situ* at 80°C in solution. The coatings exhibited good coverage on the silicon surface, but the hardness was rather low. Characterization tools including x-ray diffraction (XRD), atomic force microscopy (AFM), scanning electron microscopy (SEM), and nanoindentation were employed to achieve a better understanding of the synthesis and processing of the coatings and their relation to the mechanical properties.

**Key words:** Zirconium oxide, self-assembled monolayers (SAMs), ceramic coatings, bilayer coatings biomimetic, nanoindentation

## INTRODUCTION

Ceramics have played a key role in the advancement of recent technologies. In particular, ceramic thin films and coatings are currently being used in fuel cell electrolytes, dielectric films in semiconductor devices, thermal barrier coatings, and wear-resistant coatings.<sup>1–3</sup> In addition, ceramic films have shown a potential for protective coatings for microelectromechanical systems (MEMS) and harsh-environment electronic devices due to their good mechanical properties and inertness.<sup>4</sup>

Ceramic coatings have also been suggested as a hermetic packaging alternative for MEMS, microelectronics, and sensors in harsh and corrosive environments.<sup>5</sup> To isolate MEMS from environmental attack, high vacuum hermetic packaging is often employed. This packaging, however, not only increases the volume and weight of the devices, but also raises processing and material costs. It is estimated that hermetic packaging is responsi-

ble for 70–95% of the overall cost of a MEMS device.<sup>6</sup>

Conventional ceramic processing, however, cannot be easily implemented for surface coatings. Film cracks and interfacial delamination often occur with ceramic films because of shrinkage and thermal expansion mismatch. In addition, ceramic processing usually requires high temperatures for densification. Therefore, a major challenge to produce ceramic coatings is to find a low-temperature synthetic route with little shrinkage, as well as to accommodate the stress development during processing. Interestingly, the best example of control of ceramic processing is routinely observed in nature.<sup>7</sup> A few specific examples include eggshells, teeth, bones, and kidney stones whose growth, morphology, and composition are directed by organic matrices.<sup>8</sup>

In biological environments, biomineralization involves the controlled nucleation and growth of inorganic (ceramic) materials from aqueous solutions. Several aspects have been explored to mimic this system (called “biomimetic” synthesis) based on the premise that the tailored macromolecules in living

organisms represent a type of surface functionalization. For example, simple ionized surface functional groups mediate surface nucleation and growth.<sup>9–12</sup> In particular, a self-assembled monolayer (SAM) has been attached to functionalize the surface.

Our research has thus far focused on the synthesis of zirconia thin film/coatings grown on a SAM-coated silicon surface via a solution precursor method at low temperatures. A goal of this study is to generate a SAM coating conducive for ceramic deposition, to synthesize nanocrystalline ceramic films, and to characterize its crystallinity and mechanical properties. In particular, structural/mechanical evolution of the coating is assessed by nanoindentation.

### EXPERIMENTAL PROCEDURE

The substrates used in this study are silicon wafers (n-type, <100> single crystal; Silicon Quest International, Santa Clara, CA). Silicon wafers were cleaned with piranha solution (3 H<sub>2</sub>SO<sub>4</sub> : 1 H<sub>2</sub>O<sub>2</sub>). This acid cleaning activated the surface of the wafer and created an oxide layer necessary for a SAM deposition. The SAM coating was then deposited on the hydrolyzed silicon wafer by immersing into a trichlorosilane solution inside a vacuum sealed cell or glove box.

A variety of different surface functional groups can be processed for SAM coatings grown on silicon wafers. In this study, we focused on the SAM precursor C<sub>12</sub>H<sub>29</sub>O<sub>6</sub>PSi (which we denote “PO-SAM”; Gelest, Inc., Tullytown, PA). The SAM coatings were further hydrolyzed in HCl solution to obtain a suitable surface terminus for subsequent ceramic growth. In order to perform this, an acid hydrolysis was carried out at temperatures in the range of 65–90°C for durations of up to 2 h.

For depositing ceramic coating using a solution process, a fresh stock of 0.01 M zirconium sulfate (Zr(SO<sub>4</sub>)<sub>2</sub>·4H<sub>2</sub>O; Alfa Aesar, Ward Hill, MA) was used as a precursor solution. The substrates (SAM-coated or cleaned bare silicon samples) were submerged in this precursor solution for 24 h in a constant temperature oil bath maintained at 80°C. After a 24-h processing period, the coated samples were rinsed with distilled water and dried in a stream of nitrogen.

The SAM-coated samples and the ceramic/SAM-bilayer-coated samples were examined by a variety of characterization tools such as scanning electron microscopy (SEM), atomic force microscopy (AFM),

ellipsometry, contact angle measurement, and x-ray diffraction (XRD). In particular, mechanical properties of the coatings at different processing and annealing conditions were monitored with the aid of a nanoindenter (Hysitron TriboScope, Minneapolis, MN). Mechanical characterization can also provide a fundamental understanding for structural evolution of the ceramic precursor for various processing conditions. This instrument is coupled with an in-situ AFM imaging capability.

### RESULTS AND DISCUSSION

An SAM is a dense, oriented molecular layer composed of long chain hydrocarbon that has a surface-bonding group and a terminal group. We have thus far investigated several SAMs that have a different surface functionality, including -COOR, -SiCl<sub>3</sub>, -PO<sub>3</sub>R<sub>2</sub>, and -Br.<sup>13</sup> These SAMs were deposited on silicon substrates and were characterized for film thickness, coverage, and uniformity. When they are processed properly, the SAM surfaces are clear and do not bear any surface features by manual inspection, and appear identical to bare Si samples. Visible marks on the surface therefore indicate some contamination during the SAM preparation.

All SAM precursors have the same bonding group covalently connected to the silicon surface, but offer different surface functionality and serve as nucleation sites for subsequent ceramic growth. As a result, a major attempt has been made to create or modify the surface terminus to better match with the ceramic precursor chemistry.

It was observed that film structure and uniformity were excellent with the SAM prepared from C<sub>12</sub>H<sub>29</sub>O<sub>6</sub>PSi (PO-SAM), which produced a -PO<sub>3</sub>R<sub>2</sub> termination (surface view, Fig. 1). There exists some contamination on the surface (white dots) that may have occurred on exposure to air during the SAM characterization (Fig. 1a). It turns out that the surface can be easily contaminated or readily react with the environment. Therefore, ceramic film growth has always been processed in an isolated chamber before the SAM coating can come in contact with air.

Figure 1b revealed surface roughness of the PO-SAM grown on Si, in which a close-packed structure was visible. This AFM characterization displayed a uniform SAM coverage on the silicon surface. The thickness measured by ellipsometry was about 10

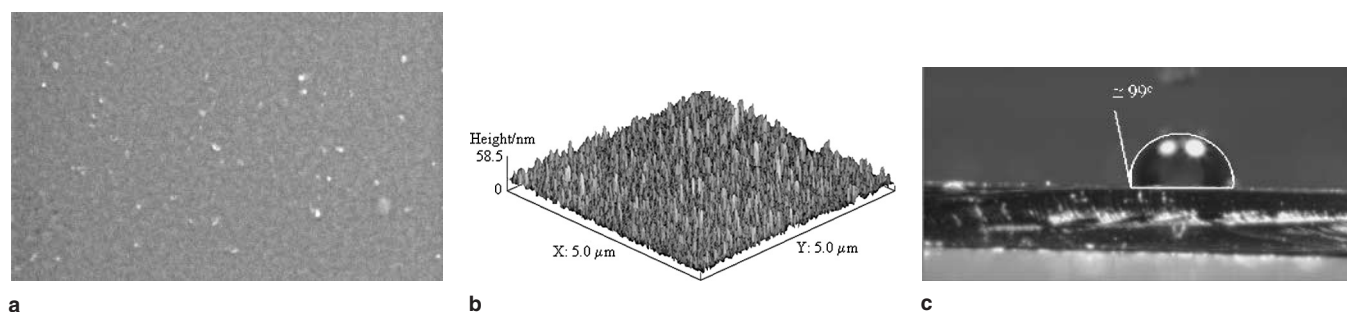


Fig. 1. Characterization of PO-SAM deposited on silicon by (a) SEM surface image, (b) AFM surface image, and (c) contact angle measurement.

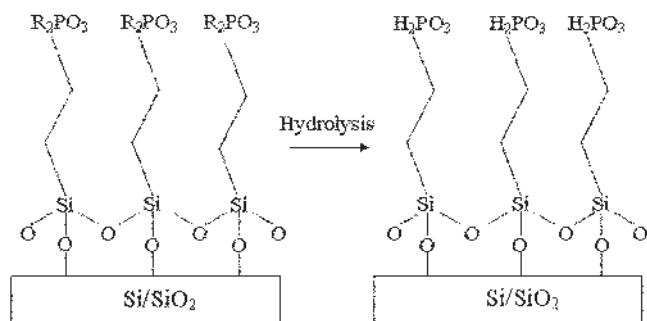


Fig. 2. Transformation of the SAM surface functionality via acid hydrolysis.

nm. The contact angle of the as-deposited PO-SAM coated samples was about  $99^\circ$ , indicating a very hydrophobic surface ( $-\text{PO}_3\text{R}_2$ ) (Fig. 1c).

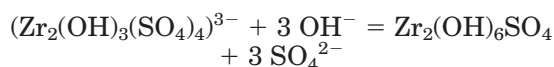
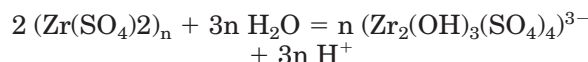
Surface modification has also been pursued to replace the ethoxy group ( $\text{R} = \text{C}_2\text{H}_5$ ) with an alcohol group prior to ceramic deposition. For this process, the aforementioned PO-SAM was hydrolyzed by  $\text{HCl}$ . The surface modification is schematically exemplified in Fig. 2. The hydrolysis process resulted in a hydrophilic surface of the SAM layer from contact angle measurements. In fact, this process is believed to provide a desirable  $-\text{PO}_3\text{H}_2$  surface, onto which the ceramic film can be nucleated and grown in a well-controlled manner.

Given that a proper organic surface is prepared on the substrate, two film growth mechanisms can be responsible for oxide growth.<sup>14</sup> The first one is due to heterogeneous nucleation occurring at the SAM-modified surface, thereby leading to directed growth of nuclei of the inorganic phase (biomimetic). This mechanism will result in strong adhesion to the selected ceramic coatings, since the organic layer surface is molecularly designed to covalently incorporate ceramic precursor molecules. The molecules are subsequently developed into a hard, ceramic surface layer. One drawback of this process is that it may only deposit a relatively thin layer (less than a couple of nanometers).

The second mechanism involves homogeneous nucleation in solution, resulting in colloidal clusters by hydrolysis and condensation reactions of the dissolved species. These clusters are then attracted to

the functional groups of the organic monolayer by electrostatic interaction. This phenomenon has been observed in transition metals such as  $\text{Zr}^{4+}$ , and depends strongly on pH. This process can lead to deposition of much thicker coatings, in which structure uniformity and control is dependent on the size of the colloidal particles.

In the experiments reported in this study, the film deposition was performed using a precursor solution of zirconium sulfate ( $\text{Zr}(\text{SO}_4)_2 \cdot 4\text{H}_2\text{O}$ ). The SAM-coated Si samples were immersed in 0.01 M precursor solution at  $80^\circ\text{C}$ . The formation of the bulk precipitate may be due to the formation of anionic species and basic sulfate precipitates, as given by



This scheme will further involve polymerization and condensation of the hydrolyzed metal ions, thereby resulting in the creation and growth of the  $\text{ZrO}_2$  nuclei.<sup>10,14,15</sup>

The coatings deposited using 0.01 M  $\text{Zr}(\text{SO}_4)_2 \cdot 4\text{H}_2\text{O}$  solution indicated strong dependence on the surface condition of the substrate. For example, the coating coverage (indicated by dark contrast) was rather poor when the ceramic precursor was deposited on cleaned, bare silicon (Fig. 3a). The coverage, however, increases when the surface has a SAM coating (Fig. 3b). This SAM has a  $-\text{PO}_3\text{R}_2$  surface functional group, and is hydrophobic, as mentioned before. Notably, a significant improvement of coverage is visible when the coating was deposited on the hydrophilic surface of the SAM (Fig. 3c). It is noted that a hydrophilic surface is not a sufficient condition for good coverage, since the bare silicon, which is very hydrophilic, does not have good coverage.

Microstructure of the coating resembles a particulate structure, as shown in the SEM images (Fig. 4). The coating consists of spherical particles over the entire surface. In this micrograph, it can be seen that the surface conditions provided by bare silicon and a hydrophobic SAM did not show a good coverage. In contrast, the hydrolyzed PO-SAM showed a

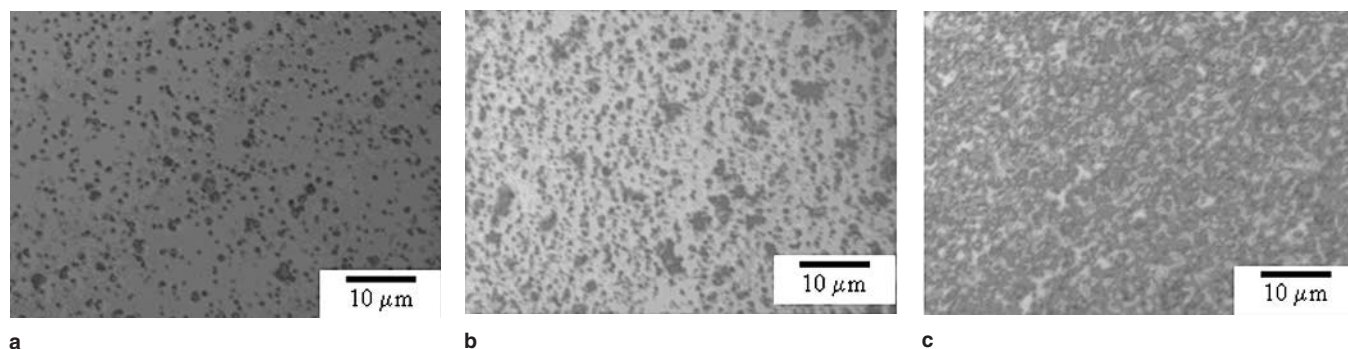


Fig. 3. Optical micrographs of the coating grown on (a) bare Si (hydrophilic), (b) PO-SAM (hydrophobic), and (c) hydrolyzed PO-SAM (hydrophilic).



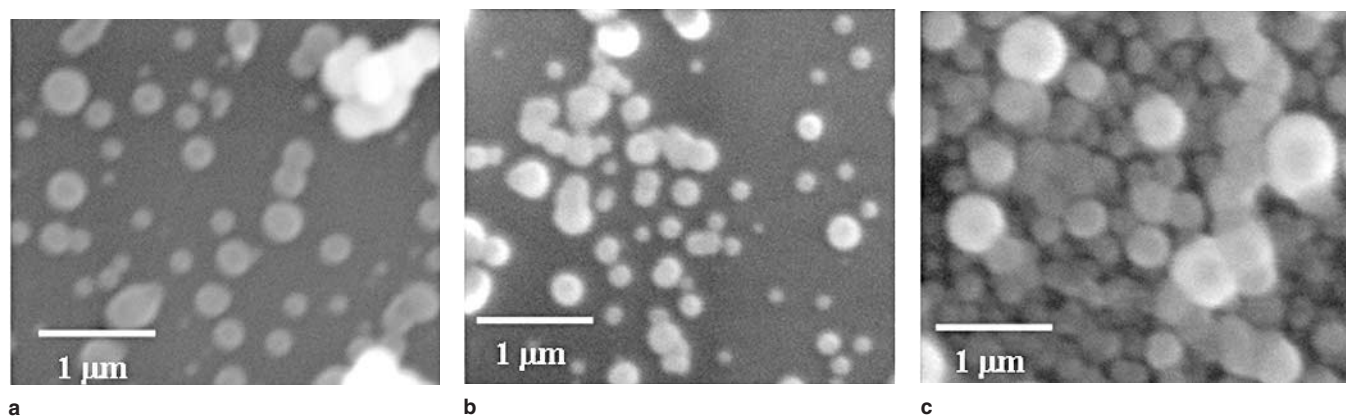


Fig. 4. SEM image of the coating grown on (a) bare Si (hydrophilic), (b) PO-SAM (hydrophobic), and (c) hydrolyzed PO-SAM (hydrophilic).

densely packed structure. In fact, this structure suggests that both heterogeneous surface nucleation and colloidal cluster formation are responsible for the growing film. Once available surface sites are occupied by the  $\text{ZrO}_2$  nuclei, the colloidal particles are attracted to the surface and are stacked onto the predeposited layers. It is also observed that the film structure is not fully dense, thereby requiring a densification mechanism in order to have protection from a variety of environmental attacks. Some “necking” areas between particles are also seen, implying a potential for further densification.

The XRD results revealed an amorphous nature of the film until the coatings were heat treated at very high temperatures (Fig. 5a). Two low-angle peaks arise from the substrate. Crystalline tetragonal (“t”) and monoclinic (“m”)  $\text{ZrO}_2$  phases are observed at 1,000°C, though the structure is still dominated by an amorphous phase.

These results are in stark contrast with the coating deposited by spin coating.<sup>13</sup> Spin coating is produced by spreading the precursor solution onto the substrate, and then drying and pyrolyzing at high temperatures. As a result, there is little chemical interaction between the precursor and the substrate

prior to pyrolysis. In this physical deposition method, we were able to detect crystalline  $\text{ZrO}_2$  formed after heat treatments between 500°C and 800°C. While this physical deposition method has the precursor decomposed into oxides at elevated temperatures, the current chemical method involves reactions in solution that retard ceramic crystallization. One possible source for this deterrence is contamination from Si and C. Our preliminary X-ray photoelectron spectroscopy (XPS) results showed that the ceramic coating indeed contains C and Si.

Mechanical properties of the ceramic coatings also support the XRD-observed structural evolution. For this purpose, nanoindentation was used to measure the hardness of the deposited coatings.<sup>16</sup> Hardness is a critical property for application of films as wear-resistant coatings. Figure 5b shows the soft nature of the particulate film. The hardness increases as the annealing temperature increases, but is still less than 3 GPa, even after heat treatment at 1,200°C. In contrast, spin-coated  $\text{ZrO}_2$  showed hardness values over 12 GPa,<sup>13</sup> which are close to those of bulk  $\text{ZrO}_2$ . This low hardness can be attributed to retardation of crystallization for  $\text{ZrO}_2$  due to contamination, as indicated by the XRD results.

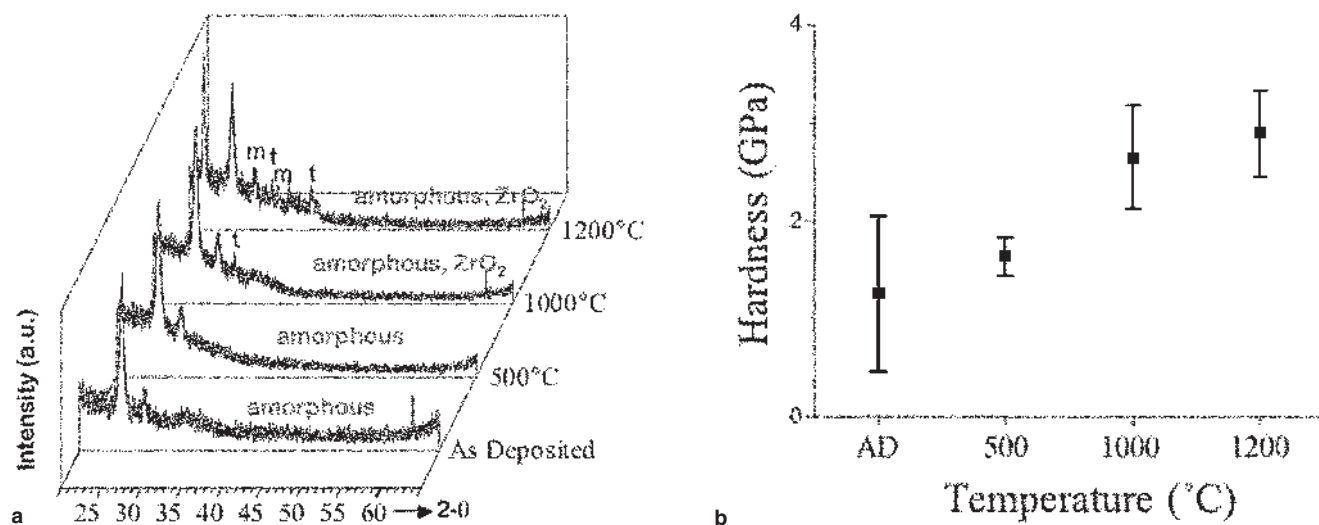


Fig. 5. (a) XRD characterization of the in-situ solution prepared coating at different annealing temperatures. (b) Its corresponding hardness.

This low mechanical strength and amorphous nature are not well understood at this point.

It is also noted that nanoindentation testing was performed on individual particles, especially on top layers of the particulate film, which may not be representative of the particles formed in deeper areas of the film. More careful mechanical characterization and cross-sectional data will be needed to better understand the properties of the ceramic coating.

As previously mentioned, the hydrolyzed (hydrophilic) SAM showed a clear advantage over the as-deposited (hydrophobic) SAM. This surface modification adds only one simple hydrolysis process, and so can be easily implemented. If we look at the microstructure of this coating carefully, however, we can observe that the bottom layer of the coating has sub-micron size particles while larger particles formed from colloidal clusters are mostly located at the surface (Fig. 6). This result indicates that the two growth mechanisms mentioned earlier operate simultaneously. Therefore, in order to have higher densification and increased uniformity, the microstructure, consisting of nanosized particles deposited on a desirable surface functionality, needs to be optimized.

This microstructure goal can be attained by accelerating surface nucleation while retarding bulk precipitation until the initial layer is entirely filled with oxide nuclei. A bulk precipitation can indeed be retarded by adding HCl to the precursor solution and controlling the process more carefully. Once the initial nucleation is completed, we will then need bulk precipitation, without which the coating thickness will not be sufficient. Controlling bulk precipitation would therefore provide a means of controlling the film thickness.

Even though we focused primarily on the in-situ chemical process for the bilayer coating at low temperature ( $<80^{\circ}\text{C}$ ), a hydrothermal method can also provide a low-temperature process using the same precursor solution. Basically, crystalline  $\text{ZrO}_2$  is formed by a hydrothermal treatment of zirconium

compound precursor, yielding isolated  $\text{ZrO}_2$  nanocrystals with the aid of autogenic pressure. The nucleation process can be very similar to the ones we have discussed above for the in-situ process. This work has only been successful for making a zirconia powder at  $\sim 125^{\circ}\text{C}$ , but may also be applied to the coating process described in this study. Consequently, this processing technique is also under investigation for the present SAM coating system.

## CONCLUSIONS

Zirconium sulfate solution was used to synthesize and process  $\text{ZrO}_2$  coatings on the PO-SAM coated Si biomimetically. The PO-SAM shows dense, uniform structure, and was used as an organic "template." The SAM functionality played an important role in determining ceramic coating characteristics. The acid-hydrolyzed SAM surface with a  $-\text{PO}_3\text{H}_2$  surface group provided a better condition for the ceramic growth than did bare silicon or the hydrophobic PO-SAM surface, leading to good coverage over the entire surface.

The resultant ceramic coating displays a porous structure with spherical particles. A neck formation between particles can also be found in some regions, thereby showing a potential for further densification. The success of the coating processed in solution at  $80^{\circ}\text{C}$  seems to have two contributions: surface nucleation and colloidal attraction. The ceramic film seemed to be amorphous and remained amorphous even with high-temperature annealing up to  $1,200^{\circ}\text{C}$ . Crystalline t- and m- $\text{ZrO}_2$  phases were, however, coexistent at high temperatures (e.g.,  $>1,000^{\circ}\text{C}$ ). Mechanical characterization by nanoindentation indicated that the ceramic coating was rather soft. More systematic studies are required to further optimize the microstructure and mechanical properties of the bilayer coating.

## ACKNOWLEDGEMENTS

This work was supported by Infotonics Technology Center Inc. (U.S. DOE Grant No. DE-FG02-02ER63410.A000), Semiconductor Research Center (Contract No. SRC No. 2003-TJ-1068), Microelectronics Design Center (Contract No. C000063), and Integrated Electronics Engineering Center (IEEC). The authors also thank X. Wang, C. McConville, and Y. Liu, Alfred University, and M. Coy, JEOL, for their help with some of the characterization.

## REFERENCES

1. G.W. Goward, *Mater. Sci. Technol.* 2, 194 (1986).
2. R.A. Miller, *J. Thermal Spray Technol.* 6, 35 (1997).
3. D.I. Pantelis, P. Psyllaki, and N. Alexopoulos, *Wear* 237, 197 (2000).
4. N. Rajan, C.A. Zorman, M. Mehregany, R. DeAnna, and R. Harvey, *Thin Solid Films* 315, 170 (1998).
5. Q. Yang, T.O. Salami, K. Chitre, S.R. Oliver, and J. Cho, *Mechanical Properties of Nanostructured Materials and Nanocomposites*, MRS Proc. (Warrendale, PA: Materials Research Society, 2004), vol. 791, pp. 105–110.
6. N. Maluf, *An Introduction to Microelectromechanical Systems* (Norwood, MA: Artech House, Inc., 2000).

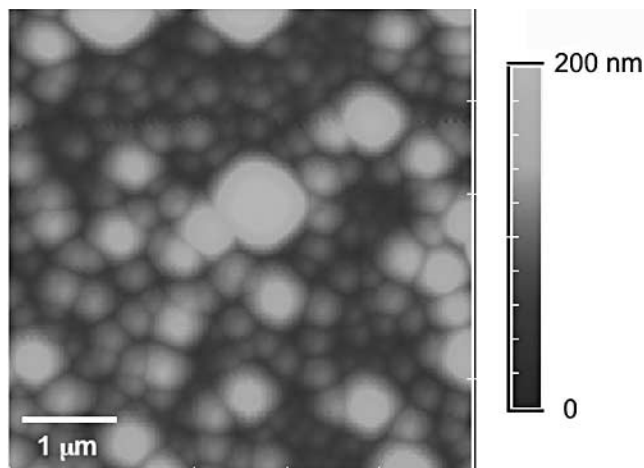


Fig. 6. AFM image of the coating structure, displaying a wide range of particle size (xy scan:  $5 \times 5 \mu\text{m}^2$ , z scan: 200 nm).

7. P. Calvert and S. Mann, *J. Mater. Sci.* 23, 3801 (1988).
8. S. Mann, in *Biomimetic Materials Chemistry*, ed. S. Mann (New York: VCH Publishers), 1996, pp. 1–40.
9. T.P. Niesen and M.R. De Guire, *J. Electroceram.* 6, 169 (2001).
10. M. Agarwal, M.R. De Guire, and A. Heuer, *J. Am. Ceram. Soc.* 80, 2967 (1997).
11. S. Supothina and M.R. De Guire, *Thin Solid Films* 371, 1 (2000).
12. H. Shin, M. Agarwal, M.R. De Guire, and A.H. Heuer, *Acta Mater.* 46, 801 (1998).
13. Q. Yang, K. Chitre, T.O. Salami, S.R. Oliver, and J. Cho, *Proc. IMECE*, ASME Int. Mechanical Engineering Congr. Expos. (New York: ASME, 2003), vol. 2, Paper No. IMECE 2003-41700.
14. J. Bill, R.C. Hoffmann, T.M. Fuchs, and F. Aldinger, *Z. Metallkd.* 93, 478 (2002).
15. B.C. Bunker, P.C. Rieke, B. J. Tarasevich, A.A. Campbell, G. E. Fryxell, G.L. Graff, L. Song, J. Liu, J. W. Virden, and G.L. McVay, *Science* 264, 48 (1994).
16. W.C. Oliver and G.M. Pharr, *J. Mater. Res.* 7, 1564 (1992).